Journal of Biomolecular NMR, 10 (1997) 77–88

J-Bio NMR 450

Assignment and secondary structure of calcium-bound human S100B*

Steven P. Smith and Gary S. Shaw**

Department of Biochemistry and McLaughlin Macromolecular Structure Facility, University of Western Ontario, London, ON, Canada N6A 5C1

Received 20 January 1997
Accepted 24 March 1997

Keywords: S100B; Calcium-bound; Secondary structure; S100 protein family

Summary

The NMR assignments of backbone ^{1}H, ^{13}C, and ^{15}N resonances for calcium-bound human S100B were completed via heteronuclear multidimensional NMR spectroscopic techniques. NOE correlations, amide exchange, $^{3}J_{H^{N}H^{\alpha}}$ coupling constants, and CSI analysis were used to identify the secondary structure for Ca-S100B. The protein is comprised of four helices (helix I, Glu^{2}–Arg^{20}; helix II, Glu^{31}–Asn^{38}; helix III, Gln^{50}–Thr^{59}; helix IV, Phe^{70}–Phe^{87}), three loops (loop I, Glu^{21}–His^{25}; loop II, Glu^{39}–Glu^{49}; loop III, Leu^{60}–Gly^{66}), and two β-strands (strand I, Lys^{26}–Lys^{28}; strand II, Glu^{67}–Asp^{69}) which form a short antiparallel β-sheet. Helix IV is extended by approximately one turn when compared to the secondary structures of apo-rat [Drohat et al. (1996) *Biochemistry*, **35**, 11577–11588] and bovine S100B [Kilby et al. (1996) *Structure*, **4**, 1041–1052]. In addition, several residues outside the calcium-binding loops in S100B undergo significant backbone chemical shift changes upon binding calcium which are not observed in the related protein calbindin D_{9k}. Together these observations support previous site-directed mutagenesis, absorption spectroscopy, and cysteine chemical reactivity experiments, suggesting that the C-terminus in Ca-S100B is important for interactions with other proteins.

Introduction

Calcium acts as a second messenger for a variety of cellular functions, including cell division and growth, muscle contraction, enzymatic activation, and cellular calcium buffering. In many of these processes, transmission of the calcium signal is through binding of the metal ion to a calcium modulatory protein. The EF-hand family is one such class of calcium-binding proteins which includes the multifunctional protein calmodulin and the muscle protein troponin C. Three-dimensional (3D) structures of these two proteins in the apo- (Finn et al., 1995; Gagné et al., 1995; Kuboniwa et al., 1995; Zhang et al., 1995) and calcium-bound (Kretsinger et al., 1986; Babu et al., 1988; Herzberg and James, 1988; Satyshur et al., 1988,1994; Finn et al., 1995; Gagné et al., 1995; Slupsky and Sykes, 1995) forms have indicated that calcium binding results in significant conformational changes, allowing them to carry out their modulatory effects via interactions with other target proteins (Gagné et al., 1995; Zhang et al., 1995).

One group of EF-hand calcium-binding proteins which has recently attracted a great deal of attention is the S100 protein family (Hilt and Kligman, 1991; Fano et al., 1995; Zimmer et al., 1995; Schafer and Heizmann, 1996). This family of low-molecular-weight (10–12 kDa) proteins comprises approximately 17 members, including S100A1 (S100a), S100B (S100b), S100A6 (calcyclin), and CALB3 (calbindin D_{9k}) (Schafer et al., 1995). Of these, S100B has been one of the most intensely studied and well characterized. First isolated from brain, S100B has subsequently been found in a variety of other tissues and has been shown to be highly conserved through a variety of species (Moore, 1965; Donato, 1991). In vitro studies have shown that phosphorylation of the neurospecific proteins tau (Baudier and Cole, 1988a,b), neuromodulin (Lin et al.,

*This work was presented at the XVIIth International Conference on Magnetic Resonance in Biological Systems, Keystone, CO, U.S.A., August 18–23, 1996.

**To whom correspondence should be addressed.

Abbreviations: MARCKS, myristoylated alanine-rich C kinase substrate; GFAP, glial fibrillary acidic protein; TNS, 6-(*p*-toluidino)naphthalene-2-sulfonic acid; CD, circular dichroism; Ca-S100B, calcium-saturated human S100B; NOE, nuclear Overhauser effect; TFE, trifluoroethanol; DTT, dithiothreitol; DTNB, 5,5'-dithiobis (2-nitrobenzoic acid); Ca-TnC, calcium-saturated troponin C.

1994; Sheu et al., 1994,1995), and MARCKS (Sheu et al., 1995) is inhibited by S100B in a calcium-dependent manner. Cellular architecture also seems to be regulated by S100B via its calcium-dependent interaction with several cytoskeletal proteins, including tubulin (Donato, 1988; Donato et al., 1989) and GFAP (Bianchi et al., 1993). In addition, elevated expression of S100B is observed in Alzheimer-afflicted patients, particularly in the regions of the brain where neuritic plaques have been localized (Griffin et al., 1989; Marshak et al., 1991; Van Eldik and Griffin, 1994). Increased S100B expression has therefore been suggested to have a role in this neuropathological disease.

S100B comprises two 91-residue β subunits, each containing one high-affinity (K_d = 7–50 μM) and one low-affinity (K_d = 200 μM) calcium-binding site (Isobe and Okuyama, 1978; Mani et al., 1983; Baudier et al., 1986b). A canonical 12-residue EF-hand calcium-binding loop (residues 61–72) is found at the acidic C-terminal, while the N-terminal contains a 14-residue (residues 18–31) pseudo-EF-hand (ψ-EF-hand) (Hilt and Kligman, 1991). Circular dichroism studies have indicated that calcium binding results in a 10% decrease in θ_{222} (Mani et al., 1983), perhaps indicating a decrease in α-helicity in the protein. Calcium binding also results in binding to phenyl sepharose and an increased fluorescence of TNS (Baudier and Gerard, 1983; Baudier et al., 1984). Previous NMR studies have identified the self-association of S100B only in the presence of calcium (Smith et al., 1996). These latter results corroborate the fluorescence work, suggesting that calcium binding to S100B induces a conformational change and exposure of a hydrophobic region. The observations further support a calcium-sensitive modulatory role for S100B via interaction with target molecules such as neuromodulin, GFAP, and tubulin. The 3D structures of apo-calcyclin (Potts et al., 1995) and, more recently, rat and bovine apo-S100B (Drohat et al., 1996; Kilby et al., 1996) have shown that, in the apo-form, these S100 proteins exist as symmetric, noncovalently linked dimers with extensive hydrophobic interactions at the dimer interface. It is clear that a better understanding of the calcium-induced structural changes in the S100 proteins will be obtained once a calcium-bound form has been elucidated. As a step towards this goal, we report the complete backbone ^1H, ^{13}C, and ^{15}N resonance assignments of calcium-saturated recombinant human S100B, which has allowed us to determine the secondary structure of this protein and correlate this with observed biological effects.

Materials and Methods

Sample preparation

$^{15}NH_4Cl$ and [$^{13}C_6$]glucose were obtained from Cambridge Isotope Laboratories Inc. (Andover, MA, U.S.A.), while [^{15}N]glycine, [^{15}N]phenylalanine, [^{15}N]alanine, trifluoroethanol-d_3 and deuterium oxide were acquired from Isotec Inc. (Miamisburg, OH, U.S.A.). Puratronic grade calcium chloride (99.9975%) was obtained from Aesar/Johnson Matthey (Brampton, ON, Canada). The auxotrophic strains DL39 GlyA DEλ and DL39 AvtA::Tn5 (LeMaster and Richards, 1988) used from selective amino acid labeling were kindly donated by L. McIntosh (University of British Columbia). All other chemicals used were of the highest purity commercially available.

Uniformly labeled recombinant human S100B was produced by overexpression in *Escherichia coli* N99 strain using M9 minimal media (Sambrook et al., 1989) containing 1.0 g/l 99% $^{15}NH_4Cl$ and 2.0 g/l 99% [$^{13}C_6$]glucose for double labeling and 1.0 g/l 99% $^{15}NH_4Cl$ for ^{15}N labeling. The backbone amides of the alanine, glycine/serine, and phenylalanine residues of S100B were selectively ^{15}N labeled and were purified as described previously (Smith et al., 1996). Electrospray mass spectrometry confirmed close to 100% isotopic enrichment of the uniformly labeled samples. Selectively ^{15}N-labeled proteins (0.5–0.6 mM) were dissolved in 81% H_2O/9% D_2O/10% TFE-d_3 containing 15 mM KCl, 5 mM DTT-d_{10}, 2.5 mM $CaCl_2$ at pH 7.10. NMR measurements of uniformly ^{15}N- and $^{13}C/^{15}N$-labeled proteins utilized 2–2.5 mM S100B samples dissolved in 81% H_2O/9% D_2O/10% TFE-d_3 containing 30 mM KCl, 10 mM DTT-d_{10}, 15 mM $CaCl_2$, 0.10 mM NaN_3 at pH 7.05. A single $^{13}C/^{15}N$ human S100B sample was used for all triple-resonance experiments.

NMR spectroscopy

All NMR experiments were acquired at 35 °C on a Varian Unity 500 MHz spectrometer equipped with a triple-resonance, pulsed field gradient (PFG) probe. The carrier frequencies used were 120 (^{15}N), 54 ($^{13}C^{\alpha}$), 43 ($^{13}C^{\beta}$), 175 ($^{13}C'$), and 4.73 (^1H) ppm. For all experiments where magnetization was detected on the amide proton, pulse field gradients were employed to select the coherence pathway for enhanced sensitivity (Kay et al., 1992).

A ^1H-^{15}N HSQC spectrum was collected using the sensitivity-enhanced method (Kay et al., 1992). The number of complex data points and spectral widths were 512, 8000 Hz (^1H) and 64, 1500 Hz (^{15}N), respectively. ^{15}N-edited NOESY-HSQC (Zhang et al., 1994) spectra were recorded with mixing times of 50 and 150 ms. The number of complex data points collected and spectral widths were 512/7000.4 Hz F3 (^1H), 32/1500 Hz F2 (^{15}N), and 128/7000.4 Hz F1 (^1H). An HNHA experiment (Vuister and Bax, 1993; Kuboniwa et al., 1994) was acquired with 512 F3 (^1H), 64 F2 (^{15}N), and 32 F1 (^1H) complex data points and used the same spectral widths as those in the ^{15}N-edited NOESY-HSQC experiments.

Sensitivity-enhanced versions of HNCACB (Wittekind and Mueller, 1993), CBCA(CO)NH (Grzesiek and Bax, 1992), and HNCO (Kay et al., 1994) triple-resonance

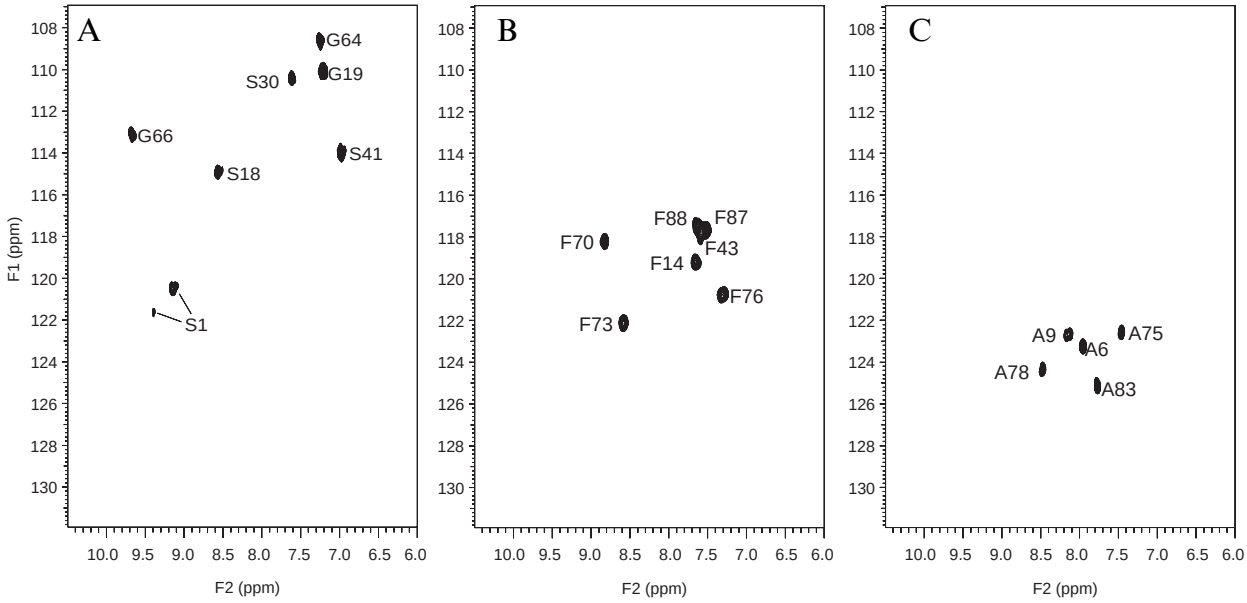

Fig. 1. ^{1}H-^{15}N HSQC spectra of selectively ^{15}N-labeled recombinant human S100B in the calcium-saturated form. The spectra show selectively labeled (A) 0.6 mM ^{15}N-glycine/serine, (B) 0.5 mM ^{15}N-phenylalanine, and (C) 0.5 mM ^{15}N-alanine S100B in the presence of 2.5 mM $CaCl_2$ and 10% (v/v) TFE-d_3 at pH 7.10 and 35 °C.

experiments were collected with the following complex data points and spectral widths: HNCACB, 512/8000 Hz F3 (^{1}H), 32/1500 Hz F2 (^{15}N), 32/7649.6 Hz F1 ($^{13}C^{\alpha/\beta}$); CBCA(CO)NH, 512/8000 Hz F3 (^{1}H), 30/1215 Hz F2 (^{15}N), 48/7287.3 Hz F1 ($^{13}C^{\alpha/\beta}$); HNCO, 512/8000 Hz F3 (^{1}H), 32/1500 Hz F2 (^{15}N), 32/1541 Hz F1 ($^{13}C'$). In all the above triple-resonance experiments, the ^{15}N chemical shift was recorded in a constant-time manner as well as the $^{13}C^{\alpha/\beta}$ chemical shift in the CBCA(CO)NH experiment.

NMRPipe and NMRDraw (Delaglio et al., 1995) were used to process all data sets on a Sun Sparc5 workstation. Linear prediction was used to double the number of planes in the F1 and F2 dimensions of the HNCACB, CBCA(CO)NH, and ^{15}N-edited NOESY-HSQC experiments. Pipp and Stapp programs (Garrett et al., 1991) were used for peak picking, spectral analysis, and NOE assignment.

$^{3}J_{H^{N}H^{\alpha}}$ coupling constants

Estimates of $^{3}J_{H^{N}H^{\alpha}}$ coupling constants were obtained from the HNHA experiment (Vuister and Bax, 1993; Kuboniwa et al., 1994). The spectrum was acquired on the uniformly ^{15}N-labeled human S100b sample and with parameters as described above. The diagonal-peak to cross-peak intensity ratio was used to calculate $^{3}J_{H^{N}H^{\alpha}}$ coupling constants as follows:

$$d_{cross}/d_{diagonal} = -\tan^2(2\pi^3 J_{H^{N}H^{\alpha}}\delta_2)$$

where $\delta_2 = 13.05$ ms. As this experiment was used only to estimate $^{3}J_{H^{N}H^{\alpha}}$, relaxation effects were not taken into consideration in the calculation of the coupling constants.

Amide hydrogen exchange

The amide proton exchange rates were measured by dissolving 12.0 mg of apo-S100B in 90% D_2O/10% TFE-d_3 containing 5 mM DTT-d_{10}. $CaCl_2$ (8 mM) was added and the sample was brought to pH 7.15. Four sensitivity-enhanced ^{1}H-^{15}N HSQC spectra were collected 10 min, 1.5 h, 6 h, and 14 h after dissolving the sample. Each acquisition took 35 min and the amide proton exchange rates were determined by following the intensities of the cross peaks over the time frame of the experiment.

Results

Our previous NMR studies indicated that recombinant human S100B had a strong salt dependence in the presence of calcium (Smith et al., 1996). At higher ionic strengths Ca-S100B self-associates, leading to increased line widths. This effect can be alleviated by the addition of a small amount of TFE in a manner similar to studies performed on calcium-saturated troponin C (Slupsky et al., 1995) and calcineurin (Anglister et al., 1993). As a result, the current work was carried out at low ionic strength and in a small amount of TFE (10%) to minimize line broadening and aggregation.

Sequential assignment strategy

As an initial approach to assigning Ca-S100B, we selectively ^{15}N labeled the backbone amides of alanine, phenylalanine, and glycine/serine residues, accounting for 22% of the protein sequence. The simplified ^{1}H-^{15}N HSQC spectra (Fig. 1) allowed us to identify the backbone amide proton and nitrogen resonances of residues

found in areas throughout the protein, including both EF-hand calcium-binding loops (Gly^{19}, Gly^{22}, Gly^{64}, and Gly^{66}), the N- and C-termini (Ser^{1}, Ala^{6}, Ala^{9}, Phe^{14}, Phe^{70}, Phe^{73}, Ala^{75}, Phe^{76}, Ala^{78}, Phe^{87}, Phe^{88}, and Ala^{83}), and the linker region (Ser^{41}, Phe^{43}). Several distinct spectral features were observed. As previously reported, two unique cross peaks were identified for Ser^{1} in the ^{15}N-glycine/serine labeled ^{1}H-^{15}N HSQC spectrum (Fig. 1A) corresponding to the N-formyl and desformyl initiator methionine forms of the protein (Smith et al., 1997). Further, the H^{N} position of Gly^{66} is shifted well downfield to a position similar to that found for analogous glycines in the calcium forms of troponin C (Krudy et al., 1992; Slupsky et al., 1995), calmodulin (Ikura et al., 1990), and calbindin D_{9k} (Kördel et al., 1989), indicative of calcium binding to these regions. In Fig. 1A only three of the four possible glycine resonances were observed. A selectively ^{15}N-labeled glycine Ca-S100B sample eliminated the possibility of overlap with a serine resonance and confirmed the absence of Gly^{22}, suggesting that this amide exchanges rapidly with water under these conditions (data not shown). A congested region having three cross peaks was observed in the ^{15}N-phenylalanine spectrum (Fig. 1B). The identification of Phe^{43}, Phe^{87}, and Phe^{88} as the aromatic residues making up this crowded area was achieved via 3D heteronuclear NMR experiments. These spectra provided 19 starting points for the sequential assignment of Ca-S100B.

A ^{1}H-^{15}N HSQC spectrum of Ca-S100B is shown in Fig. 2 with 87 of the 91 expected backbone amide proton resonances identified. In addition, six pairs of side-chain H^{N} resonances corresponding to three asparagine and three glutamine residues were observed. Only four residues, Met^{7}, Gly^{22}, Asp^{23}, and Lys^{24}, were not observed in this spectrum. The spectrum has many well-resolved cross peaks with H^{N} chemical shifts >8.6 ppm, but also exhibits a region (boxed in Fig. 2) between 7.6 and 8.4 ppm which contains severely overlapping resonances. In particular, resonances from Gln^{16} and Val^{56}; Asp^{54} and Asp^{65}; Leu^{3} and Leu^{32}; Val^{8}, Leu^{10}, Glu^{58}, Thr^{82}; and His^{15} and Asp^{63}

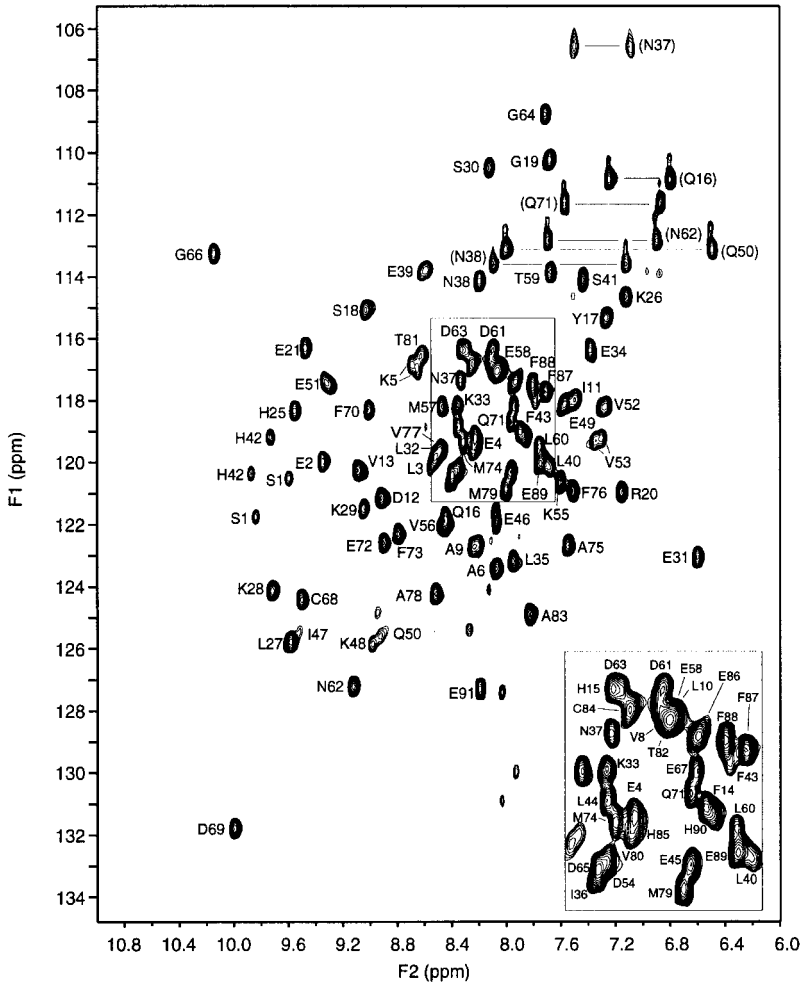

Fig. 2. ^{1}H-^{15}N HSQC spectrum of 2.5 mM calcium-saturated human S100B at pH 7.08 and 35 °C. Peaks for backbone amide protons have been assigned and are labeled with the one-letter code for the amino acid type, followed by the position in the sequence. Peaks for side-chain amide protons are connected by horizontal lines and the corresponding assignments are in parentheses. The inset is an expanded view of a crowded region where a large amount of overlap occurs and is delineated by the solid lines within the spectrum.

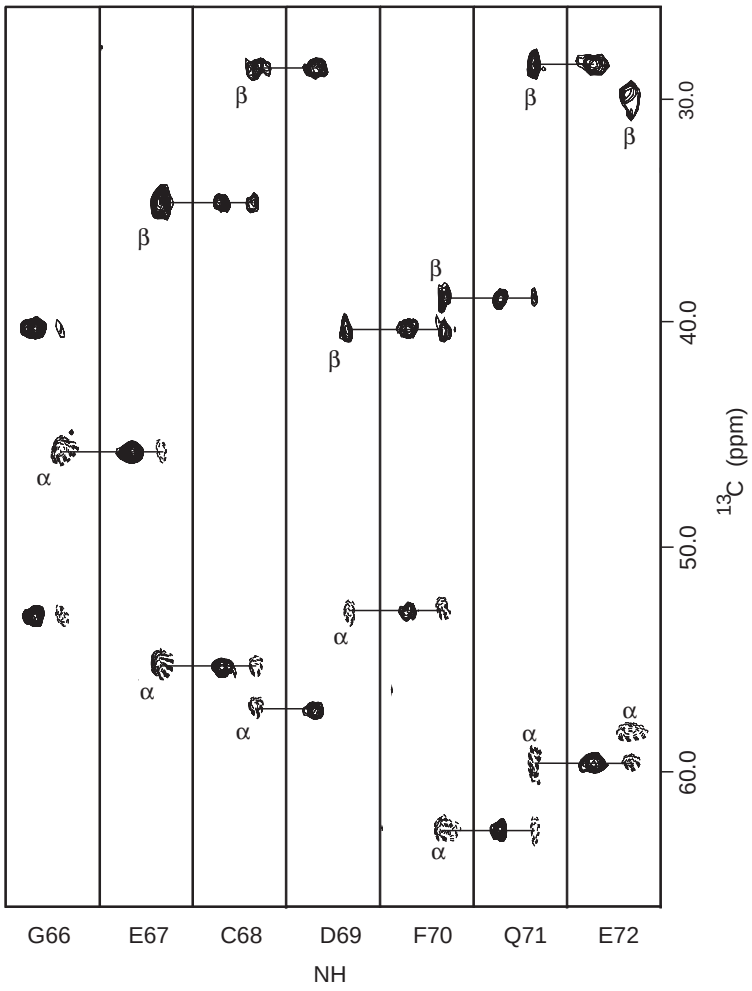

Fig. 3. Assignment of the main-chain resonances in the C-terminal calcium-binding loop of calcium-saturated human S100B using HNCACB and CBCA(CO)NH experiments. The spectra are presented as pairs of strips taken from the F3–F1 (^{1}H-^{13}C) planes of the 3D HNCACB (right) and CBCA(CO)NH (left) data sets at the F2 (^{15}N) frequencies of the indicated residues. In the HNCACB strips the intraresidue C^{α} and C^{β} correlations are labeled as α and β, respectively. Differentiation between C^{α} and C^{β} resonances was aided by their opposite phases: C^{α} resonances are negative (dashed lines) while C^{β} resonances are positive (solid lines). In many instances, weaker correlations to the C^{α} and C^{β} of the previous residue are also observed in the HNCACB spectrum. A matching of these ^{13}C chemical shifts with those observed in the CBCA(CO)NH spectrum, where correlations between the amide proton (residue i) and the C^{α} and C^{β} atoms of the previous residue (i–1) are observed, facilitates the sequential assignment as indicated by the solid lines.

had degenerate amide proton and amide nitrogen chemical shifts. Analysis of the specifically labeled data (Fig. 1B) greatly aided the identification of the phenylalanine resonances Phe[43], Phe[87], and Phe[88] which had very similar amide proton and amide nitrogen chemical shifts. A detailed analysis of the data revealed that duplicate peaks were present for residues Ser[1], Lys[5], Ser[41], and His[42], consistent with previous observations of apo-S100B and resulting from the presence of both formyl and desformyl N-terminal methionine S100B species (Smith et al., 1997). Doubling of the Val[53] resonance was also observed in the ^{1}H-^{15}N HSQC spectrum of Ca-S100B. However, unlike Ser[1], Lys[5], Ser[41], and His[42], Val[53] appeared as a single resonance in the apo-S100B ^{1}H-^{15}N HSQC spectrum. This may suggest that the Val[53] environment is somehow altered in the presence of calcium.

A knowledge of the amide proton and nitrogen chemical shifts of the glycine, serine, phenylalanine, and alanine residues of Ca-S100B from the selectively ^{15}N-labeled samples allowed initial identification in CBCA(CO)NH (Grzesiek and Bax, 1992) and HNCACB (Wittekind and Mueller, 1993) triple-resonance data and their use as starting points in the sequential assignment. The amide proton and nitrogen of residue i were correlated with the C^{α} and C^{β} of the preceding residue (i–1) using the CBCA(CO)NH experiment and matched with the intra- and interresidue $C^{\alpha/\beta}$ resonances observed in the HNCACB data. This latter experiment gave rise to 104 of a possible 180 interresidue i–1 C^{α} and C^{β} cross peaks. Regions of these spectra showing the sequential assignments of residues 66–72 are shown in Fig. 3. Further, ^{15}N-edited NOESY-HSQC spectra provided short-range $d_{NN}(i,i+1)$

TABLE 1
^{15}N, ^{13}C, AND ^{1}H RESONANCE ASSIGNMENTS FOR CALCIUM-BOUND HUMAN S100B

Residue	N	C	C^{α}	C^{β}	Others
Met^{0}		175.85	55.07	35.68	
Ser^{1a}	121.81 (9.86)	174.46	57.51 (4.75)	65.19	
Ser^{1b}	120.47 (9.62)		57.15 (4.75)	65.20	
Glu^{2}	119.99 (9.36)	177.71	59.54 (4.17)	29.45	
Leu^{3}	119.91 (8.53)	177.68	57.97 (4.20)	42.29	
Glu^{4}	119.46 (8.25)	178.81	59.49	29.78	
Lys^{5}	116.78 (8.70)	179.47	59.99 (3.93)	32.72	
Ala^{6}	123.24 (8.10)		55.13 (4.21)	18.26	
Met^{7}		178.71			
Val^{8}	116.79 (8.10)	177.69	66.97 (3.60)	31.73	
Ala^{9}	122.74 (8.25)	179.93	55.43 (4.34)	18.41	
Leu^{10}	116.76 (8.04)	178.64	58.70 (3.99)	42.22	
Ile^{11}	117.96 (7.51)		65.59 (3.71)	39.02	
Asp^{12}	120.93 (8.94)	179.64	57.68 (4.53)	41.06	
Val^{13}	120.04 (9.11)		66.58 (3.95)	31.27	
Phe^{14}	119.06 (7.87)		62.99 (3.55)	39.13	
His^{15}	116.29 (8.28)	177.91	58.20 (4.87)	28.76	
Gln^{16}	121.83 (8.46)	177.51	58.52 (3.95)	28.05	N^{ε} 111.22 (6.80, 7.24)
Tyr^{17}	115.34 (7.28)		60.92 (4.10)	40.11	
Ser^{18}	115.03 (9.04)	177.49			
Gly^{19}	110.17 (7.69)	173.53	45.62 (3.88, 4.08)		
Arg^{20}	120.92 (7.17)	177.23	59.66 (3.96)	30.85	
Glu^{21}	116.28 (9.49)		54.65 (4.63)	34.87	
Gly^{22}					
Asp^{23}					
Lys^{24}					
His^{25}	118.50 (9.57)	173.19	55.24 (4.90)	30.41	
Lys^{26}	114.55 (7.14)	174.84	55.33 (5.13)	39.02	
Leu^{27}	125.63 (9.58)	175.81	52.66 (5.14)	43.54	
Lys^{28}	124.06 (9.72)	177.61	54.93 (4.67)	33.19	
Lys^{29}	121.37 (9.06)	177.57	62.28 (3.66)	32.72	
Ser^{30}	110.76 (8.17)	177.00	60.85 (4.72)		
Glu^{31}	123.17 (6.63)		59.04 (4.17)	31.40	
Leu^{32}	120.18 (8.52)	177.29	57.48 (4.24)	42.94	
Lys^{33}	118.13 (8.39)	177.12	60.10 (3.70)	32.24	
Glu^{34}	116.32 (7.42)	177.91	59.30 (4.03)	29.10	
Leu^{35}	123.22 (7.98)	179.04	59.46 (4.05)	41.88	
Ile^{36}	120.92 (8.43)	178.31	66.84 (3.45)	38.28	
Asn^{37}	117.23 (8.36)	177.24	54.93 (4.54)	37.61	N^{δ} 106.50 (7.12, 7.51)
Asn^{38}	114.00 (8.21)	176.94	55.01 (4.85)	40.73	N^{δ} 113.16 (7.14, 8.12)
Glu^{39}	113.86 (8.63)	178.40	55.40 (5.04)	30.80	
Leu^{40}	120.06 (7.70)	177.33	53.75 (5.37)	42.52	
Ser^{41}	114.00 (7.44)	175.64	60.38 (4.46)	63.75	
$His^{42}a$	120.44 (9.92)		58.30 (4.55)	28.14	
$His^{42}b$	119.10 (9.76)		58.36 (4.61)	27.25	
Phe^{43}	117.68 (7.81)	175.11	57.39 (4.73)	40.66	
Leu^{44}	118.65 (8.38)	175.96	53.45 (4.66)	44.00	
Glu^{45}	120.00 (7.95)	175.59	56.71 (4.09)	30.40	
Glu^{46}	121.82 (8.10)		56.49 (4.07)	30.68	
Ile^{47}	125.50 (9.59)	176.36	62.06 (4.09)	38.28	
Lys^{48}	125.36 (9.03)	175.92	56.34 (4.46)	34.35	
Glu^{49}	118.15 (7.58)		55.49 (4.63)	31.71	
Gln^{50}	125.10 (8.98)	176.99	58.23 (3.87)	28.41	N^{ε} 113.51 (6.51, 8.01)
Glu^{51}	117.25 (9.32)	178.37	59.53 (4.20)	29.18	
Val^{52}	118.14 (7.28)	177.40	65.88 (3.81)	31.47	
Val^{53}	119.09 (7.33)	177.09	66.22 (3.58)	31.45	
Asp^{54}	120.28 (8.41)	178.48	57.82 (4.21)	39.86	
Lys^{55}	120.50 (7.64)	179.48	58.41 (4.16)	31.94	
Val^{56}	122.26 (8.49)	178.08	66.84 (3.56)	31.62	
Met^{57}	118.15 (8.50)	177.10	57.74 (4.24)	30.84	

TABLE 1
(continued)

Residue	N	C	C^{α}	C^{β}	Others
Glu^{58}	117.22 (8.10)	178.45	59.10 (4.05)	29.63	
Thr^{59}	113.90 (7.69)	175.10	65.98 (4.03)	68.71	
Leu^{60}	119.62 (7.81)	177.87	56.01 (4.32)	43.17	
Asp^{61}	116.30 (8.14)	176.13	54.32 (4.54)	40.26	
Asn^{62}	126.97 (9.19)	176.17	54.51 (4.79)	40.45	N^{δ} 112.16 (6.91, 7.70)
Asp^{63}	116.61 (8.37)	177.80	53.28 (4.71)	39.96	
Gly^{64}	108.88 (7.75)	175.07	47.43 (3.87, 4.04)		
Asp^{65}	120.45 (8.42)	177.23	53.63 (4.56)	40.14	
Gly^{66}	113.06 (10.12)	172.57	45.78 (3.48, 4.10)		
Glu^{67}	118.14 (7.95)	175.08	55.16 (4.82)	34.33	
Cys^{68}	124.56 (9.51)	174.64	56.72 (5.73)	27.76	
Asp^{69}	131.63 (10.01)	175.46	53.04 (5.19)	40.58	
Phe^{70}	118.17 (9.02)	176.68	62.95 (3.20)	39.25	
Gln^{71}	118.61 (7.95)	179.45	59.63 (3.73)	28.28	N^{ε} 112.13 (6.87, 7.57)
Glu^{72}	122.33 (8.94)	179.57	58.46 (4.15)	29.89	
Phe^{73}	122.31 (8.81)	176.77	60.40 (4.20)	39.37	
Met^{74}	119.52 (8.35)	178.77	55.86 (4.06)	30.09	
Ala^{75}	122.60 (7.57)	180.00	55.47 (4.08)	17.65	
Phe^{76}	120.89 (7.50)	176.47	59.73 (4.43)	38.51	
Val^{77}	119.55 (8.50)	179.59	66.66 (2.98)	31.32	
Ala^{78}	124.17 (8.56)	179.30	55.86 (3.93)	17.97	
Met^{79}	120.91 (8.02)	178.66	59.59 (4.09)	32.65	
Val^{80}	120.13 (8.37)		66.44 (3.52)	31.84	
Thr^{81}	116.74 (8.67)		68.35 (4.27)	68.73	
Thr^{82}	117.23 (8.12)	176.24	67.64 (4.05)	68.36	
Ala^{83}	125.08 (7.87)		55.12 (4.23)	17.79	
Cys^{84}	116.83 (8.31)		62.05 (4.08)	26.46	
His^{85}	119.21 (8.25)	176.09	59.89 (4.07)	29.03	
Glu^{86}	117.25 (7.91)	177.66	58.49 (3.91)	29.34	
Phe^{87}	117.69 (7.75)	176.59	59.21 (4.33)	38.98	
Phe^{88}	117.66 (7.85)	176.04	58.64 (4.43)	39.28	
Glu^{89}	119.99 (7.78)	175.60	56.61 (4.16)	30.02	
His^{90}	118.98 (7.91)	173.64	55.22 (4.63)	29.79	
Glu^{91}	127.36 (8.17)		58.23 (4.12)	30.96	

The chemical shifts were obtained at 35 °C and at pH 7.10. In each column, ^{15}N and ^{13}C chemical shifts are listed first and the corresponding H^N and H^{α} shifts follow in parentheses. The chemical shift reference used for ^{1}H and ^{13}C is the sodium salt of 3-(trimethylsilyl)-1-propane-sulfonate, and $^{15}NH_4Cl$ was used for ^{15}N.

and $d_{\alpha N}(i,i+1)$ NOE connectivities, confirming the sequential assignments made from the triple-resonance data. Strips from a 50 ms ^{15}N-edited NOESY-HSQC experiment corresponding to the beginning of the fourth helix (Fig. 4) indicate the assignment strategy of sequential NOEs. Strong $d_{NN}(i,i+1)$, weak $d_{\alpha N}(i,i+1)$, and several $d_{\alpha N}(i,i+3)$ correlations, indicative of a helical conformation, were identified in this region (Wüthrich, 1985). Particularly helpful was the identification of H^{α} chemical shifts via HNHA data since a 3D ^{15}N-edited TOCSY-HSQC experiment (Zhang et al., 1994) yielded very little signal. The backbone assignments are summarized in Table 1.

Secondary structure determination

The secondary structure in calcium-saturated human S100B was identified via NOE connectivities, CSI (Wishart and Sykes, 1994), vicinal coupling constants ($^{3}J_{H^N H^{\alpha}}$), and amide proton exchange data (Fig. 5). The results indicate that each monomer in Ca-S100B is comprised of four helices and two short antiparallel β-strands. The four helices in Ca-S100B (I, Glu^{2}–Arg^{20}; II, Glu^{31}–Asn^{38}; III, Gln^{50}–Thr^{59}; IV, Phe^{70}-Phe^{87}) were revealed by many strong and medium $d_{NN}(i,i+1)$ NOE cross peaks such as those shown for helix IV in Fig. 4. In addition, many medium-range $d_{\alpha N}(i,i+3)$ NOE correlations were noted, although this was hampered somewhat by some degenerate H^{α} resonances on adjacent residues. The $d_{\alpha N}(i,i+3)$ NOE cross peaks from all four helices were in excellent agreement with the consensus CSI. The regions of the four helices were also established by small $^{3}J_{H^N H^{\alpha}}$ coupling constants and slow amide exchange rates of residues within these regions (Fig. 5). These results and the CSI data indicated the presence of an α-helix between Ala^{78} and His^{85} even in the absence of complete $d_{\alpha N}(i,i+3)$ NOE information.

Two β-strands consisting of Lys^{26}–Lys^{28} and Glu^{67}-Asp^{69}, respectively, were located in the two proposed calcium-binding loops. These residues displayed the strong $d_{\alpha N}(i,i+1)$ and the absence of $d_{NN}(i,i+1)$ NOE correlations typically observed for β-strands (Wüthrich, 1985). Further, $^3J_{H^N H^\alpha}$ coupling constant values for residues in these regions were among the largest measured (6.81–9.74 Hz) and the calculated consensus CSI values were also consistent with the NOE data regarding the position of the β-strands. Long-range NOEs between the H^N of Lys^{29} and the H^α of Glu^{67} and the H^N of Cys^{68} and the H^α of Lys^{28} in the two strands were observed in the 50 and 150 ms NOESY-HSQC data, confirming an antiparallel β-sheet arrangement similar to that observed in the apo-structures of rat (Drohat et al., 1996) and bovine (Kilby et al., 1996) S100B and other EF-hand calcium-binding proteins. The regions Met^0–Ser^1, Glu^{21}–His^{25}, Glu^{39}–Glu^{49}, Leu^{60}–Gly^{66}, and Phe^{88}–Glu^{91} had NOEs and CSI values more representative of unstructured polypeptide. In addition, the amide protons for these residues were among the fastest to exchange.

Discussion

While a precise biological function for S100B has yet to be elucidated, in vitro binding studies have shown S100B to interact with several target proteins, including MARCKS (Sheu et al., 1995), GFAP (Bianchi et al., 1993), neuromodulin (Lin et al., 1994; Sheu et al., 1994, 1995), and tau (Baudier and Cole, 1988a,b), in a calcium-dependent manner. In addition, a bacteriophage random peptide display library has identified an S100B 'epitope', derived from the actin capping protein CapZ which the protein recognizes in the presence of calcium only (Ivanenkov et al., 1995). Based on structural information of the modulatory EF-hand calcium-binding proteins troponin C (Gagné et al., 1995) and calmodulin (Ikura et al., 1992) where target interaction requires a calcium-dependent exposure of a hydrophobic region, it has been proposed that S100B acts in a similar calcium-sensitive modulatory fashion. Previous biophysical studies corroborate this proposal (Baudier and Gerard, 1983; Mani et al., 1983; Baudier et al., 1984,1985). In our previous work we suggested that residues Phe^{14}, Phe^{73}, and Phe^{88} may be important for this hydrophobic interaction (Smith et al., 1996). Recently, the 3D structures of apo-S100B (Drohat et al., 1996; Kilby et al., 1996) and apo-calcyclin (Potts et al., 1995) have been determined. A 3D structure of Ca-S100B will therefore be a key to identifying the specific residues and structural alterations induced by calcium and will provide an insight into possible regions of interaction with target proteins.

Modifications in secondary structure

The overall secondary structure determined for human Ca-S100B is similar to that observed for apo-rat (Amburgey et al., 1995) and bovine S100B (Kilby et al., 1995)

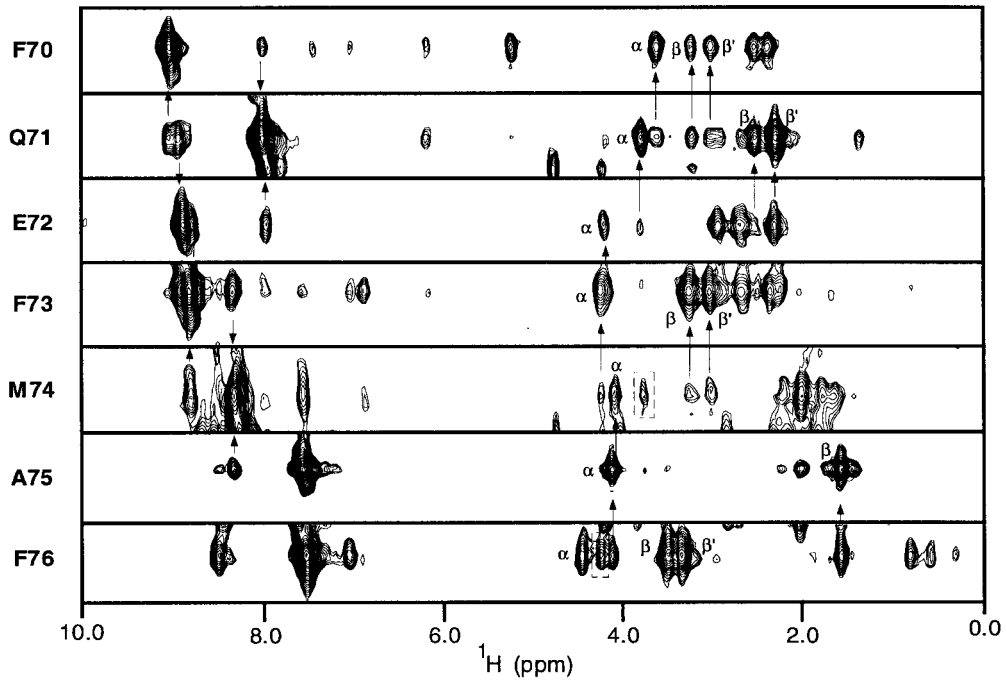

Fig. 4. Strip plots extracted from the $\tau_m = 50$ ms ^{15}N-edited NOESY-HSQC spectrum of calcium-saturated human S100B. Residues Phe^{70}–Phe^{76} are found in the IV helix of the C-terminal EF-hand calcium-binding structural motif. Sequential strong $d_{NN}(i,i+1)$ and weak $d_{\alpha N}(i,i+1)$ NOE connectivities are shown and arrows point towards the intraresidue NOE cross peaks. H^α and H^β intraresidue NOEs are labeled as α and β, respectively. Dashed boxes enclose identified $d_{\alpha N}(i,i+3)$ NOE connectivities. The diagonal cross peaks of Gln^{71}, Phe^{73}, Met^{74}, and Phe^{76} appear truncated in an attempt to exclude strings of NOEs from residues with similar amide proton chemical shifts on the same F2 (^{15}N) plane.

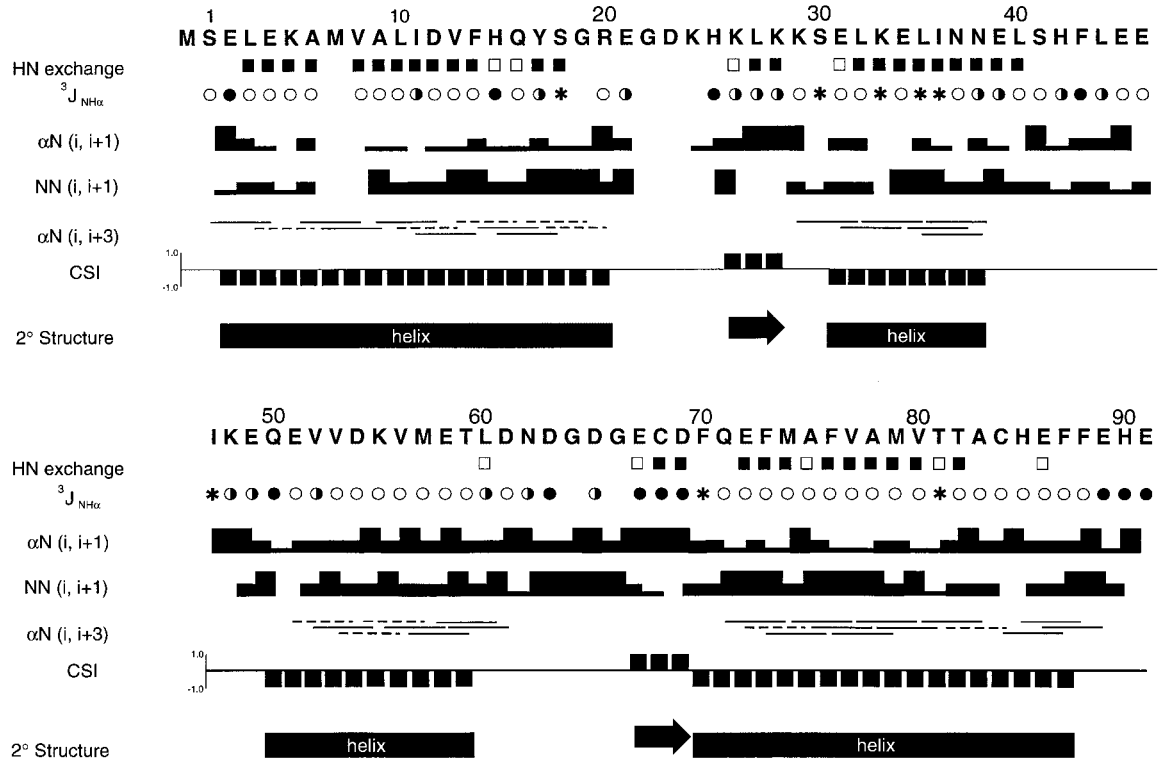

Fig. 5. Summary of sequential and medium-range NOEs involving H^N and H^α protons, backbone amide exchange rates, $^3J_{H^NH^\alpha}$ coupling constants, and CSI for calcium-saturated human S100B. For amide exchange data, full boxes indicate residues with slow exchanging amide protons (>14.5 h), empty boxes mark residues with intermediate exchanging amide protons (45 min–14.5 h), and residues with fast exchanging amide protons (<45 min) are unmarked. Residues Val[8], Leu[10], and Thr[82] have degenerate H^N and ^{15}N chemical shifts in HSQC spectra and could not be differentiated in the amide exchange data. Therefore, all three residues were identified as slow exchanging based on the presence of a peak at their corresponding H^N and ^{15}N chemical shifts after 14.5 h. Large (>8 Hz), medium (6–8 Hz), and small (<6 Hz) $^3J_{H^NH^\alpha}$ coupling constants are indicated by solid, half-shaded and empty circles, respectively, as determined from the HNHA data. Asterisks denote residues where no H^α cross peak was observed, while residues where the H^α chemical shift has yet to be identified are unmarked. The rows labeled $d_{\alpha N}(i,i+1)$ and $d_{NN}(i,i+1)$ summarize the sequential NOE cross peaks. Bar thicknesses (high, medium, and low) represent strong, medium, and weak NOE cross peaks. The row labeled $d_{\alpha N}(i,i+3)$ summarizes medium-range NOE correlations. Solid lines represent distinct $d_{\alpha N}(i,i+3)$ correlations and dashed lines identify correlations where degeneracy of C^α protons occurs. The consensus CSI ($CSI^{C^\alpha} + CSI^{C'} - CSI^{H^\alpha}$) is indicated as positive and negative bars except for residues where insufficient chemical shift information was available. These were assigned a value of zero. The derived secondary structure of calcium-saturated S100B is depicted as solid bars for helices and arrows for β-strands and identified under the appropriate residues.

and apo-calcyclin (Potts et al., 1995), as well as for calbindin D_{9k} in both the apo- (Skelton et al., 1990) and calcium forms (Kördel et al., 1989). In Ca-S100B our results show that the N-terminal pseudo-EF-hand is comprised of incoming helix I (residues Glu[2]–Arg[20]), exiting helix II (residues Glu[31]–Asn[38]) and intervening loop where calcium is coordinated. The C-terminal EF-hand comprises helix III (residues Gln[50]–Thr[59]), helix IV (residues Phe[70]–Phe[87]), and the calcium-binding loop. Two notable exceptions between the secondary structures of apo- and Ca-S100B are the lengths of helices I and IV, which are both elongated in Ca-S100B. Helix I contains two more residues (Gly[19], Arg[20]) while helix IV is extended by four and five residues, respectively (Ala[83]–Phe[87]), when compared to the bovine and rat apo-S100B structures. The change in helix I is similar to that observed for calbindin D_{9k}, where helix I is increased by one residue (Ala[16]) upon calcium binding (Skelton et al., 1994,1995). However, the extension in helix IV of Ca-S100B occurs in a region not contained in calbindin D_{9k} which is nine residues shorter than S100B. Further, these helix increases in Ca-S100B are in contrast to CD studies, where calcium binding to S100B results in a 10–15% decrease in Θ_{222} (Mani and Kay, 1983), indicating that a decrease in α-helical content does not occur. More recently, it has been shown that a change in orientation of one or more helices with respect to each other or interactions between α-helices can cause such a decrease in Θ_{222} and this may be occurring here (Manning, 1989). It is interesting that Drohat et al. (1996) have noted that the orientation of the C-terminal helices in apo-S100B differs from that in other EF-hand proteins, so calcium binding may act to reorient these helices. Alternatively, some extension of the helices in Ca-S100B could arise from the presence of 10% TFE based on its ability to stabilize helical structure. However, analysis of ^1H-^{15}N HSQC spectra of ^{15}N-phenylalanine labeled Ca-S100B in the absence and presence of 10% TFE showed only minimal proton chemical shift changes (data not

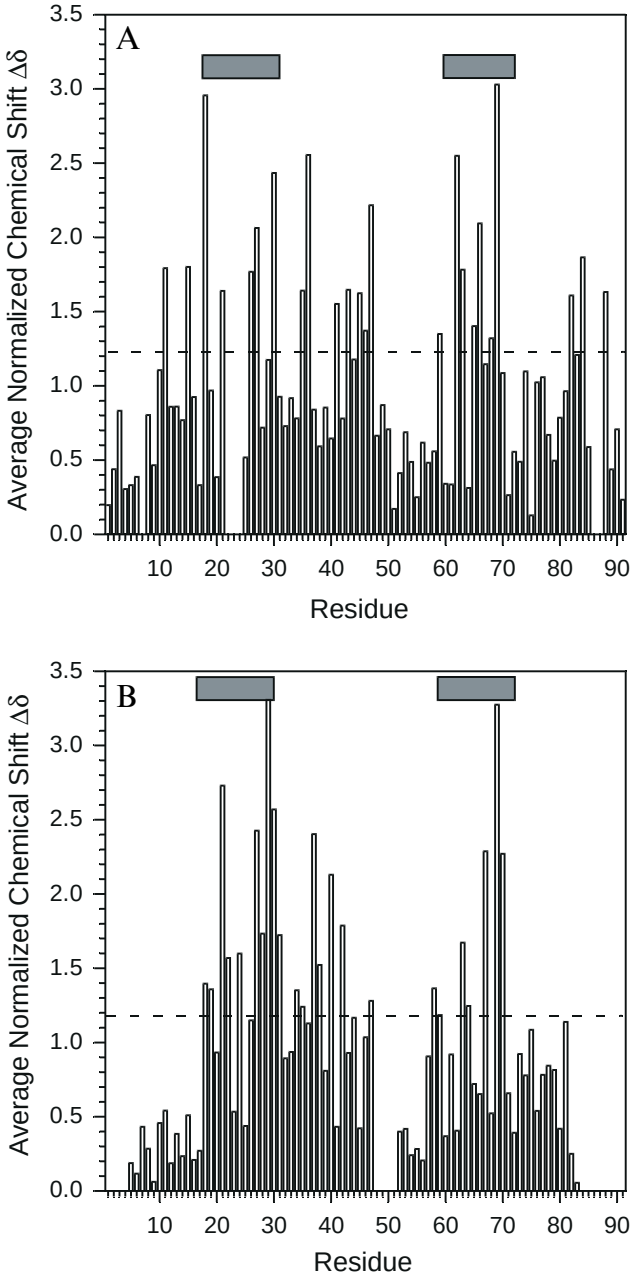

Fig. 6. Average chemical shift change along the sequence of (A) S100B (this work and unpublished data) and (B) calbindin D_{9k} (Kördel et al., 1989; Skelton et al., 1990) induced by the binding of calcium. The sequence of calbindin D_{9k} was aligned with S100B as done previously, except that a gap at position 45 of S100B was not included to preserve its sequential numbering. The chemical shift change for each residue was obtained by averaging the normalized change of the backbone HN, ^{15}N, and H^{α} chemical shifts. The normalized chemical shift change for a particular nucleus was calculated by dividing the observed chemical shift change by the average shift change for all residues. In this presentation, a value of 1 corresponds to the average change in chemical shift and a value of 0 corresponds to no change in chemical shift. Horizontal bars represent the position of the calcium-binding loops in the protein sequence. The dashed lines identify the 99% confidence levels for S100B and calbindin D_{9k}.

shown). These changes were consistent with the magnitude and direction of proton chemical shift changes observed for individual amino acids in the presence of TFE (Merutka et al., 1995).

Biological significance

The 3D structures of bovine (Kilby et al., 1996) and rat apo-S100B (Drohat et al., 1996) and apo-calcyclin (Potts et al., 1995) show extensive hydrophobic interactions involving helices I, II and IV, the linker, and C-terminal regions which maintain the dimeric interface of these S100 proteins. Hydrophobic residues involved at the dimer interface are conserved in the S100 family and include Leu^{3}, Leu^{10}, Ile^{11}, Phe^{14}, Leu^{35}, Ile^{36}, Leu^{40}, Phe^{43}, Phe^{70}, Phe^{73}, Val^{77}, and Phe^{88} (Drohat et al., 1996). These are proposed to form a common mode of association among S100 family members. An exception is the monomeric S100 protein calbindin D_{9k} which lacks the C-terminal aromatic residues (Phe^{87}, Phe^{88}) known to interact with Phe^{14} (helix I) and Phe^{70} (helix II) at the dimer interface of S100B. Although several highly conserved hydrophobic residues are found in the linker region and the C-terminus in the S100 proteins, these regions also show the least amount of sequence similarity among family members. This latter point has led to suggestions that these regions may be responsible for target protein specificity (Hilt and Kligman, 1991), although this is clearly complicated by the importance of these residues at the dimer interface in the apo-proteins.

Previously, Gagné and co-workers used a comparison of H^{N}, ^{15}N, and H^{α} chemical changes due to calcium binding to interpret structural alterations for the N-terminal of troponin C (NTnC) (Gagné et al., 1994). This approach proved very useful to show that the backbone orientation of residues Glu^{41} and Leu^{42} in the second helix changed, reflecting a calcium-induced straightening of this helix. With the backbone assignments of both Ca-S100B and apo-human S100B (unpublished results) completed, a similar chemical shift comparison was done for S100B (Fig. 6A) and the monomeric S100 protein calbindin D_{9k} (Kördel et al., 1989; Skelton et al., 1990) (Fig. 6B) to shed light on the possible different responses of these two proteins to calcium. Not surprisingly, this analysis revealed that the largest calcium-induced changes in S100B and calbindin D_{9k} occur for residues in the two calcium-binding loops. Specifically, several residues of the C-terminal EF-hands of S100B (Asn^{62}, Gly^{66}, and Asp^{69}) and calbindin D_{9k} (Gly^{59}, Val^{61}, and Ser^{62}) exhibit large calcium-induced changes. In the N-terminal pseudo-EF-hand calcium-binding loops, residues Ser^{18}, Leu^{27} and Ser^{30} (S100B) and Glu^{17}, Leu^{23}, Lys^{25} and Glu^{26} (calbindin D_{9k}) show significant trends.

Calbindin D_{9k} is 16 residues shorter than S100B, is not dimeric, and does not exhibit calcium-sensitive binding to other proteins. Therefore, it is of particular interest to compare the linker region and the N- and C-termini of these two proteins. Outside the two calcium-binding sites,

the only other region in calbindin D_{9k} to experience significant chemical shift changes is the end of helix II (Gln^{33}, Phe^{36}) and the beginning of the linker region (Ser^{38}). The lack of change on the remainder of calbindin D_{9k} is in agreement with the subtle changes exhibited by the backbone in response to calcium binding (Skelton et al., 1994,1995). In contrast, normalized chemical shift differences in S100B are noticeably altered for residues found in helix I (Ile^{11}, His^{15}), helix II (Ile^{36}), the linker (Ile^{47}), and the C-terminus (Thr^{82}, Cys^{84}, Phe^{88}). Since these changes primarily reflect backbone conformational change, it is not surprising that Thr^{82}, Cys^{84}, and Phe^{88} are affected. These are all in the region where the C-terminal helix has been extended in Ca-S100B. It is not obvious how the remaining residues are affected from this helix extension. However, it is interesting to note that Phe^{88} has intermonomer contacts with $Ile^{11'}$, $Phe^{14'}$ and $Phe^{70'}$ and Thr^{82} contacts $Phe^{70'}$ in apo-S100B (Drohat et al., 1996; Kilby et al., 1996) and apo-calcyclin (Potts et al., 1995). Further, in the apo-S100B monomer Phe^{43} interacts with Thr^{81} and Ile^{47} contacts Ala^{83}. So it would appear that a calcium-induced change in secondary structure for residues Cys^{84}–Phe^{87} might affect other residues in the Ca-S100B dimer, although at present these cannot be determined. It has been proposed that a small change in the conformation of the linker region of rat S100B due to calcium binding is required to expose Cys^{84} to solvent, presumably in part due to the interaction between the two regions (Drohat et al., 1996). The significant changes in the linker region (Phe^{43}, Ile^{47}) as well as in Cys^{84} corroborate this hypothesis. Therefore, the extension of helix IV and the changes in the linker regions may provide clues into the proposed calcium-induced change and/or exposure of regions necessary for target protein interaction.

We have modeled the region near Phe^{88} in order to assess the effect of a calcium-induced helix extension near this residue. Modeling of the helix from Ala^{83} to Phe^{87} has the effect of exposing both Phe^{87} and Phe^{88} to solvent. This observation is consistent with absorption spectroscopic studies which show that at least one phenylalanine residue becomes exposed upon calcium binding (Mani et al., 1983). Site-directed mutagenesis studies on the S100 protein p11 have also shown that Cys^{82}Gln, Tyr^{85}Ala, and Phe^{86}Ala mutations (analogous to Cys^{84}, Phe^{87}, and Phe^{88} of S100b) cause a dramatic decrease in the binding affinity of p11 for annexin II (p36) (Kube et al., 1992). In addition, previous calcium-binding studies indicate that Cys^{84} becomes more exposed in the presence of calcium due to increased reactivity with thiol-specific reagents such as DTNB, bimane, and acrylodan (Baudier and Gerard, 1983; Baudier et al., 1985,1986a). These observations are consistent with the observed changes in secondary structure between apo- and Ca-S100B whereby calcium binding to the protein induces an extension of the C-terminal helix.

Conclusions

The ^{1}H, ^{13}C and ^{15}N resonance assignments and secondary structure determination of Ca-S100B have shown that an important extension of the C-terminal helix occurs. This observation provides the first structural evidence to support biochemical experiments suggesting that the C-terminal region is important for protein–protein interactions. However, several residues in this region are also important for interactions at the dimer interface in the apo-protein. It will be important to determine whether some rearrangement at this dimer interface has occurred.

Acknowledgements

The authors would like to thank Kathy Barber and Mike Kanakos for excellent technical support. We thank Lewis Kay (University of Toronto) for advice and for providing all pulse sequences. We are grateful to Lawrence McIntosh (University of British Columbia) for the gift of auxotrophic *E. coli* strains and his suggestions for ^{15}N labeling, and to Frank Delaglio and Dan Garrett (NIH) for NMRPipe and Pipp. We also thank Stéphane Gagné (University of Alberta) for many useful discussions. This research was supported by a grant from the Medical Research Council of Canada (G.S.S.), a graduate studentship from the Alzheimer Society of London and Middlesex (S.P.S.), and an Alzheimer Society of Canada Doctoral Award (S.P.S.). Funding for the NMR spectrometer in the McLaughlin Macromolecular Structure Facility was made possible through grants from the Medical Research Council of Canada and the Academic Development Fund of the University of Western Ontario and generous gifts from the R. Samuel McLaughlin Foundation and the London Life Insurance Co. of Canada.

References

Amburgey, J.C., Abildgaard, F., Starich, M.R., Shah, S., Hilt, D.C. and Weber, D.J. (1995) *J. Biomol. NMR*, **6**, 171–179.

Anglister, J., Grzesiek, S., Ren, H., Klee, C.D. and Bax, A. (1993) *J. Biomol. NMR*, **3**, 121–126.

Babu, Y.S., Bugg, C.E. and Cook, W.J. (1988) *J. Mol. Biol.*, **203**, 191–204.

Baudier, J. and Gerard, D. (1983) *Biochemistry*, **22**, 3360–3369.

Baudier, J., Glasser, N., Haglid, K. and Gerard, D. (1984) *Biochem. Biophys. Acta*, **790**, 164–173.

Baudier, J., Labourette, G. and Gerard, D. (1985) *J. Neurochem.*, **44**, 76–84.

Baudier, J., Glasser, N. and Duportail, G. (1986a) *Biochemistry*, **25**, 6934–6941.

Baudier, J., Glasser, N. and Gerard, D. (1986b) *J. Biol. Chem.*, **261**, 8192–8203.

Baudier, J. and Cole, R.D. (1988a) *J. Biol. Chem.*, **263**, 5876–5883.

Baudier, J. and Cole, R.D. (1988b) *Biochemistry*, **27**, 2728–2736.

Bianchi, R., Giambanco, I. and Donato, R. (1993) *J. Biol. Chem.*, **268**, 12669–12674.

Delaglio, F., Grzesiek, S., Vuister, G.W., Zhu, G., Pfeifer, J. and Bax, A. (1995) *J. Biomol. NMR*, **6**, 277–293.
Donato, R. (1988) *J. Biol. Chem.*, **263**, 106–110.
Donato, R., Giambanco, I. and Aisa, M.C. (1989) *J. Neurochem.*, **53**, 566–571.
Donato, R. (1991) *Cell Calcium*, **12**, 713–726.
Drohat, A.C., Amburgey, J.C., Abildgaard, F., Starich, M.R., Baldisseri, D. and Weber, D.J. (1996) *Biochemistry*, **35**, 11577–11588.
Fano, G., Biocca, S., Fulle, S., Mariggio, M., Belia, S. and Calissano, P. (1995) *Prog. Neurobiol.*, **46**, 71–82.
Finn, B.E., Evenas, J., Drakenberg, T., Walthro, J.P., Thulin, E. and Forsén, S. (1995) *Nat. Struct. Biol.*, **2**, 777–783.
Gagné, S.M., Tsuda, S., Li, M.X., Chandra, M., Smillie, L.B. and Sykes, B.D. (1994) *Protein Sci.*, **3**, 1961–1974.
Gagne, S.M., Tsuda, S., Li, M.X., Smillie, L.B. and Sykes, B.D. (1995) *Nat. Struct. Biol.*, **2**, 784–789.
Garrett, D.S., Powers, R., Gronenborn, A.M. and Clore, G.M. (1991) *J. Magn. Reson.*, **95**, 214–220.
Griffin, W.S.T., Stanley, L.C., Ling, C., White, L., MacLeod, V., Perrot, L.J., White, C.L. and Araoz, C. (1989) *Proc. Natl. Acad. Sci. USA*, **86**, 7611–7615.
Grzesiek, S. and Bax, A. (1992) *J. Am. Chem. Soc.*, **114**, 6291–6293.
Herzberg, O. and James, M.N.G. (1988) *J. Mol. Biol.*, **203**, 761–779.
Hilt, D.C. and Kligman, D. (1991) In *Novel Calcium-Binding Proteins. Fundamentals and Clinical Implications* (Ed., Heizmann, C.W.), Springer, Berlin, Germany, pp. 65–103.
Ikura, M., Kay, L.E. and Bax, A. (1990) *Biochemistry*, **29**, 4659–4667.
Ikura, M., Clore, G.M., Gronenborn, A.M., Zhu, G., Klee, C.B. and Bax, A. (1992) *Science*, **256**, 632–638.
Isobe, T. and Okuyama, T. (1978) *Eur. J. Biochem.*, **89**, 379–388.
Ivanenkov, V.V., Jamieson, G.A., Gruenstein, E. and Dimlich, R.V.W. (1995) *J. Biol. Chem.*, **270**, 14651–14658.
Kay, L.E., Keifer, P. and Saarinen, T. (1992) *J. Am. Chem. Soc.*, **114**, 10663–10665.
Kay, L.E., Xu, G.Y. and Yamazaki, T. (1994) *J. Magn. Reson.*, **A109**, 129–133.
Kilby, P.M., Van Eldik, L.J. and Roberts, G.C.K. (1995) *FEBS Lett.*, **363**, 90–96.
Kilby, P.M., Van Eldik, L.J. and Roberts, G.C.K. (1996) *Structure*, **4**, 1041–1052.
Kördel, J., Forsén, S. and Chazin, W.J. (1989) *Biochemistry*, **28**, 7065–7074.
Kretsinger, R.H., Rudnick, S.E. and Weissman, L.J. (1986) *J. Inorg. Biochem.*, **28**, 289–302.
Krudy, G.A., Brito, R.M.M., Putkey, J.A. and Rosevear, P.R. (1992) *Biochemistry*, **31**, 1595–1602.
Kube, E., Becker, T., Weber, K. and Gerke, V. (1992) *J. Biol. Chem.*, **267**, 14175–14182.
Kuboniwa, H., Grzesiek, S., Delaglio, F. and Bax, A. (1994) *J. Biomol. NMR*, **4**, 871–878.
Kuboniwa, H., Tjandra, N., Grzesiek, S., Ren, H., Klee, C.B. and Bax, A. (1995) *Nat. Struct. Biol.*, **2**, 768–776.
LeMaster, D.M. and Richards, F.M. (1988) *Biochemistry*, **27**, 142–150.
Lin, L.-H., Van Eldik, L.J., Osheroff, N. and Norden, J.J. (1994) *Mol. Brain Res.*, **25**, 297–304.
Mani, R.S. and Kay, C.M. (1983) *Biochemistry*, **22**, 3902–3907.
Mani, R.S., Shelling, J.G., Sykes, B.D. and Kay, C.M. (1983) *Biochemistry*, **22**, 1734–1740.
Manning, M.C. (1989) *J. Pharm. Biomed. Anal.*, **7**, 1103–1119.
Marshak, D.R., Pesce, S.A., Stanley, L.C. and Griffin, W.S.T. (1991) *Neurobiol. Aging*, **13**, 1–7.
Merutka, G., Dyson, H.J. and Wright, P.E. (1995) *J. Biomol. NMR*, **5**, 14–24.
Moore, B.W. (1965) *Biochem. Biophys. Res. Commun.*, **19**, 739–744.
Potts, B.C.M., Smith, J., Akke, M., Macke, T.J., Okazaki, K., Hidaka, H., Case, D.A. and Chazin, W.J. (1995) *Nat. Struct. Biol.*, **2**, 790–796.
Sambrook, J., Fritsch, E.F. and Maniatis, T. (1989) *Molecular Cloning: A Laboratory Manual*, Cold Spring Harbor Laboratory Press, Cold Spring Harbor, NY, U.S.A.
Satyshur, K.A., Rao, S.T., Pyzalska, D., Drendel, W., Greaser, M. and Sundaralingam, M. (1988) *J. Biol. Chem.*, **263**, 1628–1647.
Satyshur, K.A., Pyzalska, D., Greaser, M., Rao, S.T. and Sundaralingam, M. (1994) *Acta Crystallogr.*, **D50**, 40–49.
Schafer, B.W., Wicki, R., Englekamp, D., Mattei, M.G. and Heizmann, C.W. (1995) *Genomics*, **25**, 638–643.
Schafer, B.W. and Heizmann, C.W. (1996) *Trends Biochem. Sci.*, **21**, 134–140.
Sheu, F.-S., Azmitia, E.C., Marshak, D.R., Parker, P.J. and Routtenberg, A. (1994) *Mol. Brain Res.*, **21**, 62–66.
Sheu, F.-S., Huang, F.L. and Huang, K.-P. (1995) *Arch. Biochem. Biophys.*, **316**, 335–342.
Skelton, N.J., Forsén, S. and Chazin, W.J. (1990) *Biochemistry*, **29**, 5752–5761.
Skelton, N.J., Kördel, J., Akke, M., Forsén, S. and Chazin, W. (1994) *Nat. Struct. Biol.*, **1**, 239–245.
Skelton, N.J., Kördel, J. and Chazin, W.J. (1995) *J. Mol. Biol.*, **249**, 441–462.
Slupsky, C.M., Kay, C.M., Reinach, F.C., Smillie, L.B. and Sykes, B.D. (1995a) *Biochemistry*, **34**, 7365–7375.
Slupsky, C.M., Reinach, F.C., Smillie, L.B. and Sykes, B.D. (1995b) *Protein Sci.*, **4**, 1279–1290.
Slupsky, C.M. and Sykes, B.D. (1995) *Biochemistry*, **34**, 15953–15964.
Smith, S.P., Barber, K.R., Dunn, S.D. and Shaw, G.S. (1996) *Biochemistry*, **35**, 8805–8814.
Smith, S.P., Barber, K.R. and Shaw, G.S. (1997) *Protein Sci.*, **6**, 1110–1113.
Van Eldik, L.J. and Griffin, W.S.T. (1994) *Biochim. Biophys. Acta*, **1223**, 398–403.
Vuister, G. and Bax, A. (1993) *J. Am. Chem. Soc.*, **115**, 7772–7777.
Wishart, D. and Sykes, B. (1994) *J. Biomol. NMR*, **4**, 171–180.
Wittekind, M. and Mueller, L. (1993) *J. Magn. Reson.*, **B101**, 171–180.
Wüthrich, K. (1985) *NMR of Proteins and Nucleic Acids*, Wiley, New York, NY, U.S.A.
Zhang, M., Tanaka, T. and Ikura, M. (1995) *Nat. Struct. Biol.*, **2**, 758–767.
Zhang, O., Kay, L.E., Olivier, J.P. and Forman-Kay, J.D. (1994) *J. Biomol. NMR*, **4**, 845–858.
Zimmer, D.B., Cornwall, E.H., Landar, A. and Song, W. (1995) *Brain Res. Bull.*, **37**, 417–429.